

Electronic Supplementary Information (ESI)

UV-curable fluoropolymers crosslinked with functional fluorescent dyes: the way to multifunctional thin-film luminescent solar concentrators

Diego Pintossi¹, Alessia Colombo², Marinella Levi¹, Claudia Dragonetti², Stefano Turri¹, and Gianmarco Griffini^{1*}

¹*Department of Chemistry, Materials and Chemical Engineering “Giulio Natta”, Politecnico di Milano, Piazza Leonardo da Vinci 32, 20133 Milano, Italy.*

²*Department of Chemistry, Università degli Studi di Milano, Via Golgi 19, 20133 Milano, Italy.*

*corresponding author:

email: gianmarco.griffini@polimi.it

Content

| | |
|---|-----|
| Synthesis of the organic dye..... | S2 |
| UV-curable coating formulations | S4 |
| Wettability behavior of the UV-curable fluorinated coating..... | S5 |
| Luminescent system applied on temperature-sensitive plastic substrates..... | S6 |
| Figures of Merit (FoM)..... | S7 |
| Optical properties of luminophores in solution and in film..... | S8 |
| Thermogravimetric analysis in nitrogen..... | S9 |
| LSC device – PV parameters..... | S10 |
| Current-voltage characteristic curves of solar cell and LSC..... | S11 |
| PV cell – External Quantum Efficiency..... | S12 |
| Thermogravimetric analysis on aged LSC..... | S13 |
| Differential scanning calorimetry on aged LSC..... | S14 |

Synthesis of the organic dye

1,6,7,12-Tetrachloro-3,4:9,10-perylene dianhydride (1)

In a 100 ml three-necked flask equipped with a reflux condenser 3,4:9,10-perylene tetracarboxylic dianhydride (1 g, 2.55 mmol) and iodine (170 mg, 0.67 mmol) were dissolved in chlorosulfonic acid (10 ml). The mixture was heated to 70 °C for 5 h. The reaction mixture was then poured into an ice-water mixture and the insoluble product was collected by filtration. The crude product was dried under vacuum and used without purification. Yield 2.3 g (64.2%).

N,N'-bis(2,6-diisopropylphenyl)-1,6,7,12-tetrachloro-3,4:9,10-perylenetracarboxdiimide (2)

At room temperature to a mixture of compound **1** (200 mg, 0.37 mmol) in 1-propanoic acid (2.5 mL), 2,6-diisopropylaniline (350 μ l, 1.86 mmol) was added. The mixture was heated to 140 °C for 24 h and then was neutralized with a saturated solution of NaHCO₃. The product was extracted with dichloromethane and the organic phase was washed twice with distilled water and dried over sodium sulfate. The solvent was removed under reduced pressure and the crude product purified by column chromatography on silica gel (eluent: hexane/CH₂Cl₂ 1:1.) to afford **2** (4.2 g, 91%).

¹H-NMR (400 MHz; CDCl₃) δ ppm: 8.80 (4H, s), 7.57 (2H, t, *J* = 7.76 Hz), 7.42 (4H, d, *J* = 7.76 Hz), 2.82-2.76 (4H, m), 7.24-7.22 (m, 24H). MS(FAB⁺): *m/z* 849.

4-vinylphenol: To a suspension of Ph₃P (3g, 11.4 mmol) in toluene (25 mL) was added CH₃I (1.56g, 11.4 mmol), to give a white suspension which was stirred for 12 h. The desired product CH₃PPh₃I was separated by filtration as white solid, washed with hexane and dried *in vacuo*. *t*-BuOK (695 mg, 6.15 mmol) was added to a solution of CH₃PPh₃I (1.49g, 3.69 mmol) in THF (7.45 mL) and after 1h a solution of 4-hydroxybenzaldehyde (301 mg, 2.5 mmol) in THF (2mL) was slowly added. The resulting mixture was stirred at room temperature for 1h and then was quenched with water and extracted with AcOEt. The organic layer was dried with Na₂SO₄ and the solvent was removed under reduce pressure. The crude product was purified by flash chromatography using hexane/AcOEt 4:1 as eluent affording the desired product in 85% yield.

¹H-NMR (400 MHz; MeOD) δ ppm: 7.27 (2H, d, *J* = 8.48 Hz), 6.75 (2H, d, *J* = 8.48 Hz), 6.63 (1H, dd, *J* = 17.61 Hz, *J* = 10.91 Hz), 5.56 (1H, d, *J* = 17.61 Hz), 5.04 (1H, d, *J* = 10.91 Hz).

1,6,7,12-Tetrakis(4-vinylphenoxy)-N,N'-(2,6-diisopropylphenyl)perylene-3,4,9,10-tetracarboxdiimide (3): In a 100 mL flask, under nitrogen atmosphere tetrachloroperylene-tetracarboxdiimide **2** (300 mg, 0.35 mmol) was stirred overnight at 110 °C in NMP (17.5 mL) in presence of 4-vinylphenol (252 mg, 2.1 mmol) and anhydrous K₂CO₃ (145 mg, 1.05 mmol). The reaction mixture was cooled to room temperature and poured into 2N HCl (160 mL). The product was extracted with AcOEt and the organic phase washed three times with water (100 mL), and dried and dried over Na₂SO₄. The crude product was purified by flash chromatography (eluent: Hexane:CH₂Cl₂ 1:4) to give red solid **3** in 85% yield.

¹H-NMR (400 MHz; CD₂Cl₂) δ ppm: 8.24 (4H, s), 7.43 (2H, t, *J* = 7.7 Hz), 7.40-7.32 (16H, m), 7.00 (4H, d, *J* = 8.12 Hz), 6.73 (4H, dd, *J* = 17.56 Hz, *J* = 10.91 Hz), 5.73 (4H, d, *J* = 17.61 Hz), 5.26 (4H, d, *J* = 10.91 Hz), 2.74-2.72 (4H, m), 1.38-1.24 (24H, m).

¹³C-NMR (100 MHz; CD₂Cl₂) δ ppm: 163.59, 156.09, 155.42, 146.35, 136.12, 134.67, 129.88, 128.19, 124.39, 123.35, 122.71, 120.83, 120.27, 113.86, 30.07, 29.43, 24.05.

UV-vis (CH₂Cl₂) λ_{max} = 574 nm (ε = 31973 M⁻¹cm⁻¹), λ_{max} = 450 nm (ε = 14041 M⁻¹ cm⁻¹). MS(FAB⁺): *m/z* 1182.

Anal. Calcd for C₈₀H₆₆N₂O₈: 81.20 C, 5.62 H, 2.73 N; Found: 81.28 C, 5.64 H, 2.72 N.

UV-curable coating formulations

A preliminary investigation on different coating formulations was carried out to select the most promising coating material for LSC application. The selection was based on two main criteria: hydrophobicity (i.e., water contact angle as high as possible) and optical transmittance (as high as possible). The following table summarizes the results of this preliminary screening.

Table S1 Alternative formulations investigated in the preliminary phase of this work. Water contact angle values present an error equal to $\pm 2\%$ of the reported value. Y and N stand for yes and no, respectively.

| Lumeta | PFA | PFPE-UDM | Water contact angle | Transparent |
|--------|--------|----------|---------------------|-------------|
| [%] | [%] | [%] | [°] | [-] |
| 68.6% | 29.4% | 2.0% | 111.5 | N |
| 69.3% | 29.7% | 1.0% | 111.3 | N |
| 78.4% | 19.6% | 2.0% | 111.2 | Y |
| 58.8% | 39.2% | 2.0% | 114 | N |
| 97.0% | 0.0% | 3.0% | 110.1 | Y |
| 60.0% | 40.0% | 0.0% | 91.2 | N |
| 70.0% | 30.0% | 0.0% | 90 | N |
| 0.0% | 98.0% | 2.0% | 123.9 | Y |
| 0.0% | 99.0% | 1.0% | 122 | Y |
| 98.0% | 0.0% | 2.0% | 109.1 | Y |
| 100.0% | 0.0% | 0.0% | 88.9 | Y |
| 0.0% | 0.0% | 100.0% | 113.9 | Y |
| 0.0% | 100.0% | 0.0% | 122.4 | Y |
| 30.0% | 70.0% | 0.0% | 113.5 | N |
| 0.0% | 95.0% | 5.0% | 122.4 | Y |
| 50.0% | 50.0% | 0.0% | 94 | N |
| 40.0% | 60.0% | 0.0% | 119 | N |
| 9.5% | 85.7% | 4.8% | 120 | N |
| 14.3% | 81.0% | 4.8% | 121 | N |
| 42.9% | 52.4% | 4.8% | 120 | N |
| 71.4% | 23.8% | 4.8% | 107 | Y |
| 78.4% | 19.6% | 2.0% | 108 | Y |

Wettability behavior of the UV-curable fluorinated coating

Table S2 Optical contact angle and surface energy values for the crosslinked fluorinated matrix prior to and after aging.

| | $\theta_{\text{H}_2\text{O}}$ [°] | $\theta_{\text{CH}_2\text{I}_2}$ [°] | θ_{Nujol} [°] | Surface Energy [mN/m] | Polar component [mN/m] | Dispersive component [mN/m] |
|------------------|--------------------------------------|---|--------------------------------|--------------------------|------------------------------|-----------------------------------|
| Pristine coating | 119.4 ± 0.7 | 100.7 ± 0.6 | 90.9 ± 0.8 | 8.58 | 0.74 | 7.84 |
| Aged coating | 120.1 ± 0.4 | 99.1 ± 0.7 | 89.7 ± 0.5 | 9.07 | 0.54 | 8.53 |

Video S1. Wettability behavior of the new UV-curable fluorinated system upon deposition of a water droplet. For comparison, the behavior of an uncoated glass substrate is also shown.

Video S2. Cleanability behavior of an uncoated glass substrate upon deposition of a dispersion of carbon black in water (1 wt.%) to simulate atmospheric dirt.

Video S3. Cleanability behavior of the new UV-curable fluorinated system presented in this work upon deposition of a dispersion of carbon black in water (1 wt.%) to simulate atmospheric dirt.

Luminescent system applied on temperature-sensitive plastic substrates

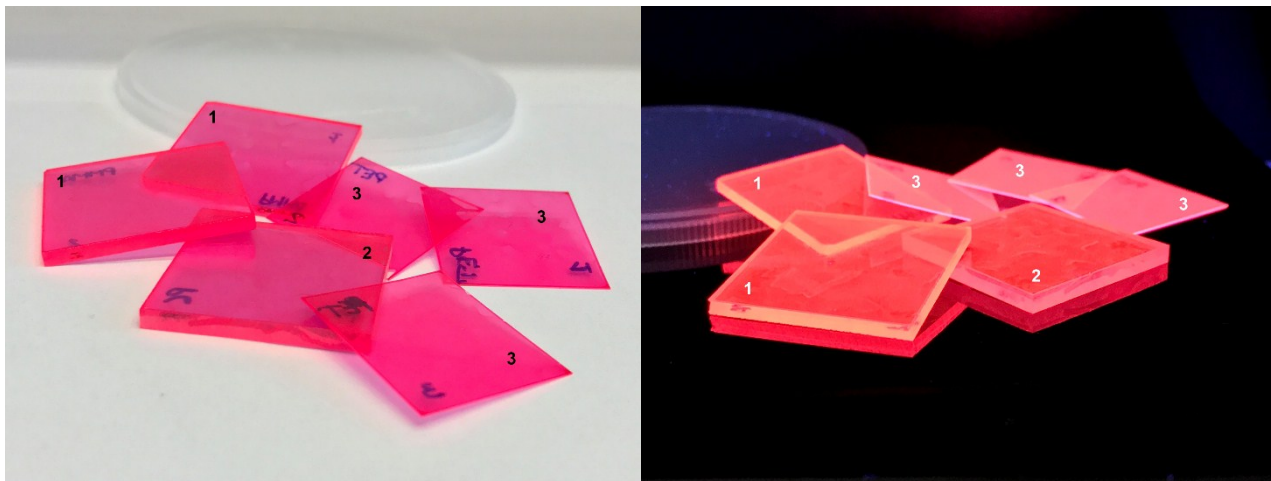


Figure S1 XL-red based luminescent system applied on **1** poly(methylmethacrylate) (PMMA), **2** polycarbonate (PC), and **3** polyethylene terephthalate (PET). (left) under ambient lighting, (right) irradiated with a 365 nm UV lamp.

Figures of Merit (FoM)

LQY (luminescence quantum yield) is a measure of the efficiency of the absorption and emission processes performed by the dye. Ideally, LQY should be 100% and it is given by:

$$LQY = \frac{\text{number of emitted photons}}{\text{number of absorbed photons}}$$

ASM (absorption spectral matching) is a measure of the match between the absorption of the dye and the spectrum of the photons that are not absorbed by the OPV device, therefore its ideal value is 100%. ASM is given by:

$$ASM = \frac{\int Abs(\lambda)AM1.5G(\lambda)[1 - EQE(\lambda)]d\lambda}{\int AM1.5G(\lambda)[1 - EQE(\lambda)]d\lambda}$$

ESM (emission spectral matching) is a measure of the match between the emission of the dye and the spectral response of the OPV device. Its ideal value is 100%. ESM is given by:

$$ESM = \frac{\int Em(\lambda)EQE(\lambda)d\lambda}{\int Em(\lambda)d\lambda}$$

RO (radiative overlap) is a measure of the overlap between the absorption and emission spectra of the dye. In the case of LQY lower than unity, RO constitutes a photon loss mechanism. Therefore, its ideal value is 0%. RO is given by:

$$RO = \frac{\int Abs(\lambda)Em(\lambda)d\lambda}{\int Em(\lambda)d\lambda}$$

PA (parasitic absorption) is a measure of the overlap between the absorption spectrum of the dye and the spectrum of the photons that are efficiently absorbed by the OPV device. Its ideal value is 0%. PA is given by:

$$PA = \frac{\int Abs(\lambda)AM1.5G(\lambda)EQE(\lambda)d\lambda}{\int AM1.5G(\lambda)EQE(\lambda)d\lambda}$$

Table S3 Calculated FoM values for the two dyes considering their absorption and emission spectra, together with the EQE of the solar cell.

| | RO | PA | ESM | ASM | LQY |
|--------|------|-----|------|------|------|
| | [%] | [%] | [%] | [%] | [%] |
| LR305 | 15.7 | 1.4 | 99.5 | 66.3 | > 90 |
| XL-red | 17.2 | 1.5 | 99.5 | 75.2 | > 90 |

Optical properties of luminophores in solution and in film

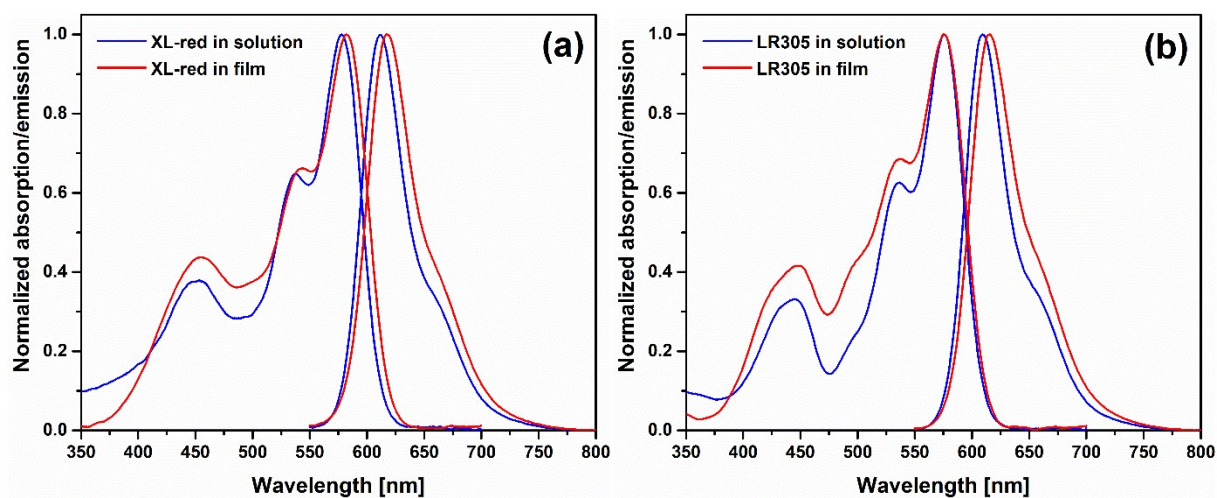


Figure S2 UV-vis absorption and fluorescence emission spectra of (a) XL-red and (b) LR305 in solution and in film. Excitation wavelength for the fluorescence spectra was 445 nm.

As shown in Figure S2, incorporation of XL-red in the polymer matrix and subsequent UV-curing is found to yield a (5 nm) red-shift of emission spectra compared to the emission in solution. Such bathochromic shift can also be observed on UV-cured luminescent coatings doped with LR305 control dye and is likely the result of a different aggregation state of the dye molecules in the solid film compared to the solution, originating from a different solvation effect

Thermogravimetric analysis in nitrogen

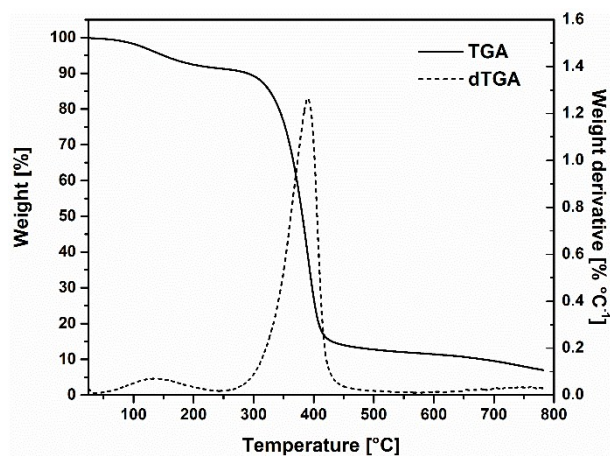


Figure S3 Weight loss and differential weight loss curves for the luminescent system in nitrogen.

LSC device – PV parameters

The performance of the LSC devices was evaluated on the basis of the following characteristic quantities [41].

1. The power conversion efficiency of the LSC device η_{LSC} , defined as:

$$\eta_{LSC} = FF \frac{V_{OC}(I_{SC}/A_{LSC})}{P_{IN}} \quad (\text{Equation S1})$$

where FF (-) is the fill factor, I_{SC} (mA) is the short circuit current and V_{OC} (V) is the open circuit voltage extracted from the PV cells attached to the LSC waveguide, A_{LSC} (cm²) is the area of the LSC top surface, and P_{IN} (mW cm⁻²) is the incident solar power density.

2. The optical efficiency of the LSC device η_{opt} , defined as:

$$\eta_{opt} = \frac{\eta_{LSC}}{\eta_{PV}} \quad (\text{Equation S2})$$

where η_{PV} is the power conversion efficiency of the PV cell under front face direct illumination.

3. The concentration factor C , defined as:

$$C = \eta_{opt} G \quad (\text{Equation S3})$$

where G is the geometric gain of the LSC device, defined as:

$$G = \frac{A_{LSC}}{A_{PV}} \quad (\text{Equation S4})$$

where A_{PV} is the total PV cell surface area present in the LSC.

Current-voltage characteristic curves of solar cell and LSC

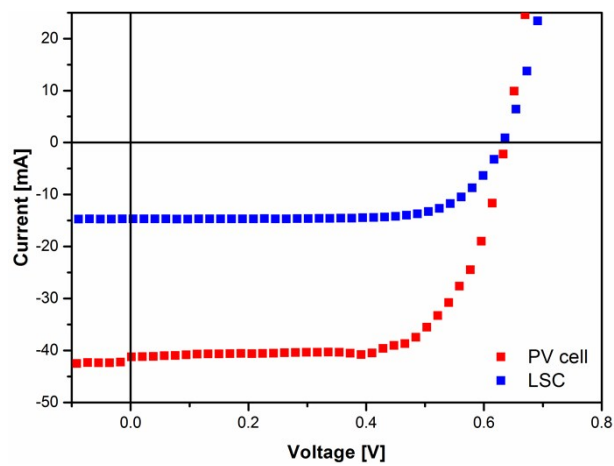


Figure S4 Representative I-V curves for (red) PV cell and (blue) LSC device.

PV cell – External Quantum Efficiency

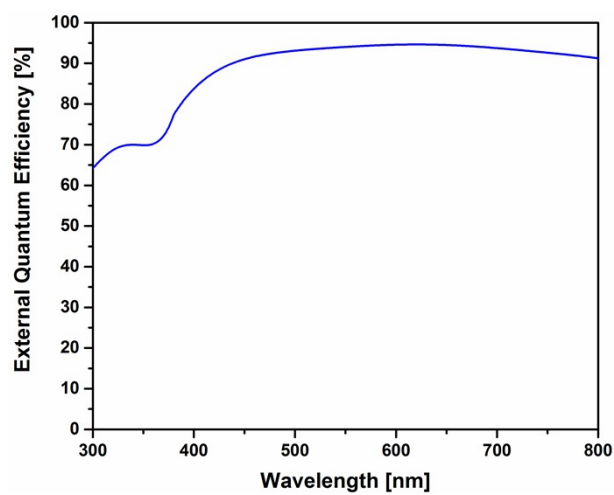


Figure S5 Representative external quantum efficiency (EQE) plot for a PV cell used in LSC fabrication.

Thermogravimetric analysis on aged LSC

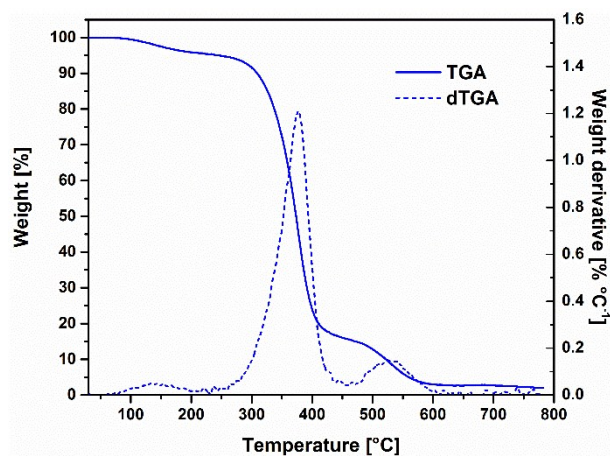


Figure S6 Weight loss and differential weight loss curves for the aged luminescent system in air.

Differential scanning calorimetry on aged LSC

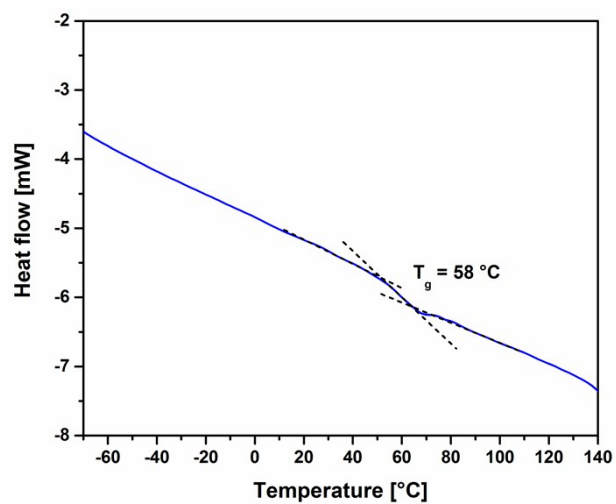


Figure S7 Differential scanning calorimetry for the aged luminescent system.